Chapter 4

Thermal Properties of Hemp Fiber Reinforced Plant-Derived Polyamide Biomass Composites and their Dynamic Viscoelastic Properties in Molten State

Yosuke Nishitani, Toshiyuki Yamanaka,
Tetsuto Kajiyama and Takeshi Kitano

Additional information is available at the end of the chapter

http://dx.doi.org/10.5772/64215

Abstract

To further enhance the mechanical, thermal, and tribological properties of short natural fiber-reinforced biopolymer composites, it is very critical to understand thermal properties of these biomass composites and their dynamic viscoelastic properties in the molten state. The aim of this study is to experimentally investigate the thermal properties of hemp fiber filled plant-derived polyamide 1010 composites and their dynamic viscoelastic properties in the molten state. It was found that the addition of HF with PA1010 has a strong influence on the thermal properties such as DMA, TGA, and DSC. HF is very effective for improving the thermal and mechanical properties. The effect of alkali treatment on the dynamic viscoelastic properties of the HF/PA1010 composites in the molten state differs according to whether alkali treatment uses silane coupling agent or not. The viscoelastic properties of $NaClO_2$ are higher than those of NaOH. Silane coupling agents have a remarkable influence on rheological properties such as storage modulus, loss modulus, and complex viscosity in the low angular frequency region in the molten state, temperature dependences of rheological properties, and relationship between the phase angle and complex modulus. These rheological behaviors are also strongly influenced by the type of silane coupling agents.

Keywords: thermal properties, dynamic viscoelastic properties, plants-derived polyamide, biomass composites, hemp fiber

1. Introduction

Biopolymers and biomass polymer composites are drawing extensive interest not only as a solution for growing environmental threats but also as a solution for the depletion of petroleum in recent years [1–4]. In addition, the supply of raw materials is becoming increasingly unstable as many biopolymers are made from edible biomass such as corn. In order to solve these problems, new engineering materials made of 100% inedible plant-derived materials are strongly required. Meanwhile, the investigation of short natural (plant) fibers such as banana fiber, flax fiber, hemp fiber, ramie fiber, and sisal fiber used for reinforced biopolymer composites have attracted great interest in recent decades [4–8]. These natural fibers have some ecological advantages over inorganic fibers such as carbon and glass fibers as they are renewable, light, recyclable, and biodegradable and can be incinerated [9]. In previous studies, we conducted the development of new engineering materials such as structural materials and tribomaterials (for mechanical sliding parts such as bearing, cum, gear, and seal) based on all plant-derived materials. In particular, we investigated the rheological, mechanical, and tribological properties of natural fiber-reinforced biopolymer composites such as hemp fiber (HF)-reinforced plant-derived polyamide 1010 (PA1010) biomass composites [10–17]. PA1010 was made from sebacic acid and decamethylenediamine, which are obtained from plant-derived castor oil [18]. As castor oil is not used for food, there is no competition with human food consumption. It was found that the mechanical and tribological properties of these composites are improved when filled with hemp fibers and surface-treated using silane coupling agent. However, in order to further enhance the mechanical, thermal, and tribological properties of the short natural fiber-reinforced biopolymer composites, it is very important to understand the thermal properties of these biomass composites and their dynamic viscoelastic properties in molten state such as process ability, heat resistance, crystallinity, internal adhesion, internal microstructures, and changes and structure–property relationships [19–21]. The aim of this study is to experimentally investigate the thermal properties of hemp fiber-filled plant-derived polyamide 1010 composites and their dynamic viscoelastic properties in the molten state.

2. Thermal properties of hemp fiber-reinforced plant-derived polyamide 1010 biomass composites

2.1. Introduction

Natural fiber-reinforced plant-derived polymer biomass composites are environment friendly to a large extent and have unique performances. However, since the interfacial adhesion between the natural fiber and matrix polymer is generally poor, these biomass composites exhibit poor mechanical properties [4, 11, 22]. Interfacial adhesion can be enhanced and the mechanical properties of these composites improved by suitable surface treatment. Most fibers are pretreated before they are used as secondary phases in composite materials. The effects of the surface treatment on the mechanical properties of these biomass composites have been

http://dx.doi.org/10.5772/64215

studied for the last two decades [3–8, 10, 11, 15–17, 22]. In particular, chemical methods such as alkali treatment (mercerization), silane treatment, and graft copolymerization and physical methods such as the corona treatment and the plasma treatment have been investigated in this field. However, only a few studies have been published on the effects of surface treatment on thermal properties of these biomass composites [14, 22–27]. The majority of natural fibers have low degradation temperatures below 200°C, which make them inadequate for processing with thermoplastics at temperatures above 200°C [27]. To further enhance the mechanical, thermal, and tribological properties of the natural fiber-reinforced biopolymer composites, it is very critical to understand the thermal properties such as heat resistance, crystallinity, internal adhesion, internal microstructures, changes, and structure–property relationships of these materials. The aim of this study is to improve the performance of all inedible plant-derived materials for new engineering materials such as structural materials and tribomaterials. Thermal properties such as dynamic mechanical analysis (DMA), thermogravimetric analysis (TGA), and differential scanning calorimetry (DSC) of hemp fiber-filled inedible plant-derived polyamide 1010 biomass composites were investigated experimentally.

2.2. Materials and methods

The materials used in this study were surface-treated hemp fiber-reinforced plant-derived polyamide 1010 biomass composites (HF/PA1010). Plant-derived polyamide 1010 (PA1010, Vestamid Terra DS16, Daicel Evonik Ltd., Japan) was used as the matrix polymer. PA1010 was made from sebacic acid and decamethylenediamine which are obtained from plant-derived castor oil [18]. Hemp fiber (HF, ϕ50–100 μm, Hemp Levo Inc., Japan) was used as a reinforcement fiber. The volume fraction of fiber V_f was fixed with 20 vol.%. HFs were precut into 5-mm-long pieces and were surface-treated by two methods: (a) alkali treatment by sodium hydroxide (NaOH) solution and (b) surface treatment using aminosilane coupling agents (S1, A-1120, 3-(2-aminoethylamino) propyltrimethoxy silane, Momentive Performance Materials Inc., USA). Alkali treatment using NaOH was employed as follows: 5% NaOH solution was placed in a stainless beaker. Then chopped HFs were added into the beaker and stirred well. This was kept at room temperature for 4 h. The fibers were then washed thoroughly with deionized water to remove excess NaOH sticking to the fibers. The alkali-treated HFs by NaOH (HF-A) were dried on air for 12 h and in a vacuum oven at 80°C for 5 h. Amino silane coupling agent was used for surface treatment. The treatment of HFs with the concentration of 1 wt.% of amino silane coupling agent was carried out in deionized water and stirred continuously for 15 min. Then, the fibers were immersed in the solution for 60 min. The surface-treated hemp fibers (HF-S1) were removed from the solution and dried in air for 12 h and in a vacuum oven at 80°C for 5 h. All the components were dried for 12 h at 80°C in a vacuum oven beforehand until the moisture level was below 0.2%, and then dry blended in a small bottle, and subsequently, the melt was mixed at 85 rpm and 220°C on a twin screw extruder (TEX-30, Japan Steel Works, Ltd., Japan). After mixing, the extruded strands of various HF/PA1010 composites were cut into 5-mm-long pieces by the pelletizer and dried again at 24 h at 80°C in a vacuum oven. Various shaped samples for various experiments were injection molded (NS20-A, Nissei Plastic Industrial, Japan). The molding conditions were as follows: cylinder temperatures of 220°C, mold (cavity) temperature of 30°C, and the injection rate of

13 cm^3/s. In addition, 2-mm-thick sheets were compression-molded under the conditions of 220°C, 3 min, and 5 MPa and cut into 5 mm × 40 mm × 1 mm-shaped specimen for measurement and dynamic mechanical analysis. To maintain the drying conditions of specimens for all measurements, they were kept in accordance with JIS K 6920–2 for at least 24 h at 23°C in desiccators after molding. Thermal properties such as dynamic mechanical analysis (DMA), thermogravimetric analysis (TGA), and differential scanning calorimetry (DSC) were evaluated. The storage modulus E', loss modulus E'', and loss tangent ($\tan\delta = E''/E'$) of the composites were measured as a function of temperature (from −100 to 200°C) using a DMA equipment (RSA3, TA instrument Japan, Inc., Japan) with a tensile fixture at a frequency of 1 Hz. Thermogravimetric analysis (TGA) was carried out in a TGA equipment (Thermo plus EVO2, Rigaku Co. Ltd., Japan). The samples used for the TGA were cut from injection-molded coupon specimens into small pieces weighing 10 mg. TGA measurement was programmed for heating from 40 to 400°C with a heating rate of 10°C/min. The differential scanning calorimetry (DSC) was measured by a DSC equipment (DSC-50, Shimadzu Co. Ltd., Japan). The samples used for the DSC were prepared like those for TGA (5 mg). The DSC measurement was scanned from −90 to 230°C with a constant heating rate of 10°C/min.

2.3. Dynamic mechanical analysis (DMA)

First, the dynamic mechanical analysis of surface-treated hemp fiber-filled polyamide 1010 biomass composites (HF/PA1010 biomass composites) is discussed. The storage modulus E' and loss tangent $\tan\delta$ (= Loss modulus E''/ Storage modulus E') are plotted as a function of temperature T for neat PA1010 (100%), untreated HF-filled PA1010 composites (HF/PA1010), HF treated by NaOH-filled systems (HF-A/PA1010), HF treated by amino silane coupling agent (S1)-filled ones (HF-S1/PA1010), and HF treated by NaOH and S1 filled ones (HF-A-S1/PA1010) in **Figure 1(a)** (E' vs. T) and **Figure 1(b)** ($\tan\delta$ vs. T), respectively. The E' of various HF/PA1010 biomass composites is higher than that of neat PA1010, indicating that HF has a strong reinforcing effect on the elastic properties of PA1010. The E' of various HF/PA1010 ones in low-temperature region less than about 50°C, which is the glass transition temperature T_g of PA1010, is the same level in spite of the kind of surface treatment. However, the E' of HF/PA1010 ones in the high-temperature region of >50°C decreases in the following sequence: HF/PA1010 (untreated) > HF-A/PA1010 > HF-A-S1/PA1010 > HF-S1/PA1010. The $\tan\delta$ curves (**Figure 1(b)**) exhibit two relaxation peaks. The first peak between at 40 and 60°C represents the glass transition temperature T_g of PA1010 and the composites, and the second one between −80 and −60°C shows the relaxation arising from the hydrogen bonds between the PA1010 chains [28]. The relaxation peak at the high-temperature region of the HF/PA1010 composites shifts slightly toward high temperature although various HF/PA1010 biomass composites are at the same level regardless of the surface treatment method. On the contrary, the relaxation peak at the lower-temperature region of neat PA1010 does not shift with the addition of HF; however, those of various surface-treated HF/PA1010 biomass composites are small in comparison with neat PA1010. In general, those of rigid fiber-filled polymer composites shift toward higher temperature due to the restriction on the movement of the polymer chains [28]. In short, flexible fibers such as the natural fiber employed in this study show the same

http://dx.doi.org/10.5772/64215

tendency. The mechanisms of how the addition of HF affects the relaxation peak at the low-temperature region of composites needs to be studied further.

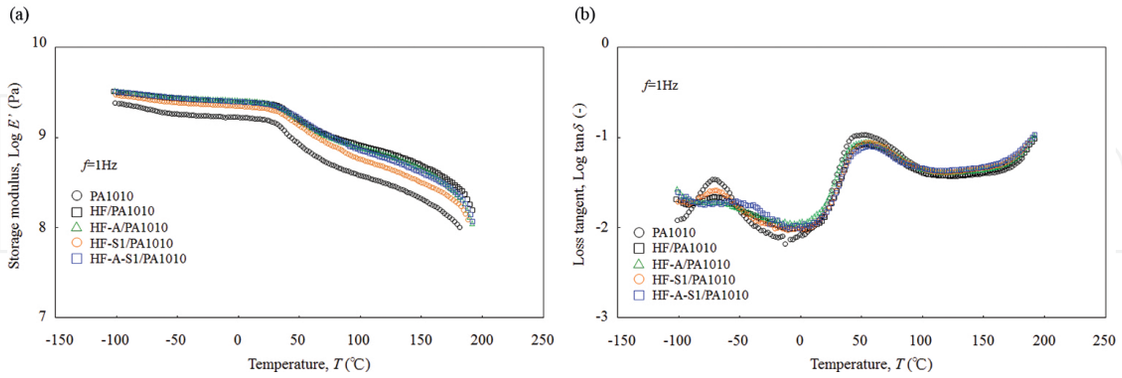

Figure 1. Dynamic mechanical properties as a function of temperature for various HF/PA1010 biomass composites. (a) Storage modulus and (b) loss tangent.

2.4. Thermogravimetric analysis (TGA)

The thermogravimetric analysis (TGA) of various surface-treated HF/PA1010 biomass composites has been discussed. **Figure 2** shows the TG curves (the weight as a function of temperature *T*) of various HF/PA1010 biomass composites. The weight of neat PA1010 is higher than that of various HF/PA1010 biomass composites over the whole temperature range. The TG curve of various HF/PA1010 biomass composites shows the evidence of two weight loss processes, while that of neat PA1010 is only one weight loss process. The first weight loss process between 80 and 200°C is attributed to the dehydration of HF as well as the thermal degradation of lignin and hemicellulose [22, 27]. The second weight loss process at about 300°C is explained in terms of the decomposition of cellulose in HF. The TG curves of various surface-

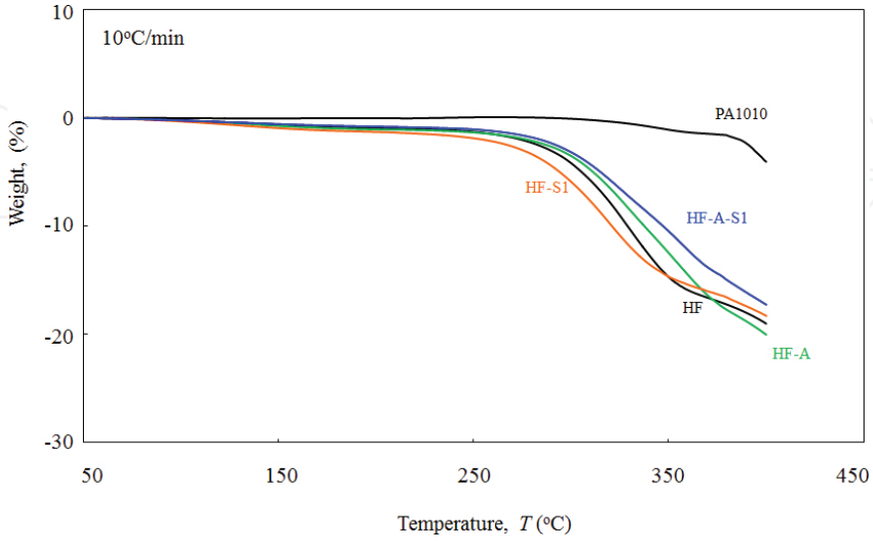

Figure 2. Thermogravimetric curves of various HF/PA1010 biomass composites.

treated HF/PA1010 biomass composites decrease in the following order: HF-A-S1/PA1010 > HF-A/PA1010 > HF/PA1010 > HF-S1/PA1010. This indicates that HF treated with the combination of NaOH and amino silane (S1) is more effective for improving the heat resistance of the HF/PA1010 biomass composites.

2.5. Differential scanning calorimetry (DSC)

The crystal form of the polymer has a strong influence on the mechanical properties of the polymer composites. Differential scanning calorimetry (DSC) was employed to evaluate the effects of the surface treatment of fiber on the crystallization behavior of HF/PA1010 biomass composites. **Figure 3** shows the DSC 1st heating (**Figure 3(a)**) and 2nd heating (**Figure 3(b)**) curves obtained at 10°C/min rate, respectively. DSC 1st heating curves in **Figure 3(a)** show a melting peak each curve, although DSC 2nd heating curves in **Figure 3(b)** have two melting peaks. This may be explained by the following mechanisms: it was pointed out recently by Li et. al. [29] that the appearance of multiple melting peaks in DSC run is probably due to rearrangement of the lamella since the polyamide crystals can be easily thickened by annealing. It is considered that the same phenomenon occurs for PA1010 used in this study. T_{m1}, which is the melting point in the lower temperature side in DSC 2nd heating curves, is attributed to the thin lamellae formed during cooling, and T_{m2}, which is in the higher ones, is attributed to the melting of the thickened crystals during the heating and annealing process. Parameters such as the melting point T_m, T_{m1}, and T_{m2} and the heat of fusion ΔH_f calculated from DSC curves for various PA1010 biomass composites are listed in **Table 1**. T_m in 1st heating curves shifts to lower temperatures when filled with the HF, and ΔH_f also decreases when HF is filled. The effect of surface treatment of fiber on the T_m and ΔH_f of HF/PA1010 biomass composites has complex behavior according to the type of the surface treatment. T_m of alkali treatment by NaOH (HF-A/PA1010 composites) shifts to higher temperature, while T_m of surface treatment by silane coupling agent (HF-S1/PA1010 composites) shifts to lower temperature. T_m of the composites surface-treated by both alkali treatment and silane coupling agent (HF-A-S1/PA1010 composites) has the immediate value between HF-A/PA1010 and HF-S1/PA1010 composites. On the contrary, ΔH_fs of HF-A/PA1010 and HF-S1/PA1010 composites are higher

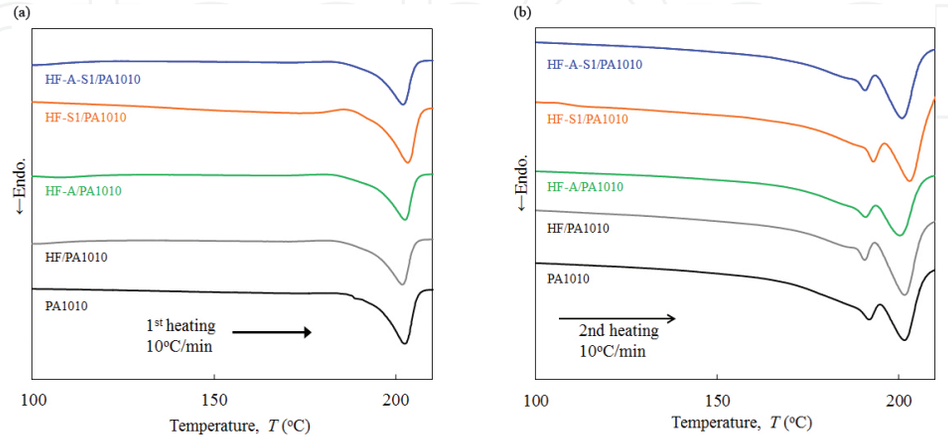

Figure 3. DSC curves of various HF/PA1010 biomass composites. (a) 1st heating and (b) 2nd heating.

http://dx.doi.org/10.5772/64215

than that of HF/PA1010 composites although ΔH_f of HF-A-S1/PA1010 composites is lower than that of HF/PA1010 composites. T_{m1}, $T_{m2,}$ and ΔH_f in 2nd heating curves also have complex behavior, and these values basically decrease with filling the HF and alkali treatment, although the values slightly increase with the surface treatment by silane coupling agent. The behavior may be due to factors such as changes in crystal form with the alkali treatment and silane coupling agent treatment caused by changing in the interfacial interaction between HF and PA1010.

	1st heating		2nd heating		
	T_m (°C)	ΔH_f (J/g)	T_{m1} (°C)	T_{m2} (°C)	ΔH_f (J/g)
PA1010	203.0	18.5	192.0	201.5	38.2
HF/PA1010	201.7	14.6	190.6	201.7	34.5
HF-A/PA1010	202.4	15.3	190.9	200.4	31.4
HF-S1/PA1010	201.5	17.7	193.0	203.0	44.0
HF-A-S1/PA1010	201.9	14.5	190.9	201.0	36.6

Table 1. Parameters calculated from the DSC curves for various HF/PA1010 biomass composites.

3. Effect of alkali treatment on dynamic viscoelastic properties of hemp fiber-reinforced plant-derived polyamide 1010 biomass composites in molten state

3.1. Introduction

The interfacial adhesion between natural fiber and matrix polymer can be enhanced and the mechanical properties of natural fiber-reinforced polymer biomass composites improved by suitable surface treatment, because the interfacial adhesion between the natural fiber and matrix polymer is generally poor as mentioned earlier. The alkali treatment (mercerization) is a chemical treatment for natural fiber, which is most commonly used to reinforce thermoplastic and thermoset [3, 4, 16, 22, 24]. An important modification resulting from the alkali treatment is the disruption of hydrogen bonding in the network structure, thereby increasing surface roughness. This treatment removes a certain amount of lignin, hemicellulose, wax, and oils covering the external surface of fiber cell wall, depolymerizes cellulose, and exposes the short length crystallites. Therefore, strong effects, such as increase of the surface roughness resulting in better mechanical interlocking and increase in the number of possible reaction sites, can be expected from this treatment. Many authors have investigated the influence of alkali treatment on the various mechanical and chemical properties of natural fiber-reinforced polymer biomass composites [3, 4, 16, 22, 24]. However, although these biomass composites undergo various flows during processing by flow molding such as injection, extrusion, and compression, generally the effect of the alkali treatment on processing properties has not been studied enough [12, 30]. It is critical to understand the rheological behavior of these biomass composites

in the molten state to understand the process ability, internal microstructures, changes, and structure–property relationships of these materials so as to further enhance the mechanical, thermal, and tribological properties of all plant-derived polymer-based biomass composites. Recently, we studied the effect of surface treatment, specifically alkali treatment with silane coupling agent, on the rheological properties of these biomass composites. The purpose of this study is to report the effect of alkali treatment on the dynamic viscoelastic properties of hemp fiber-reinforced plant-derived polyamide 1010 biomass composites in the molten state under oscillatory flow. Four types of surface treatments such as (a) alkali treatment by sodium hydroxide solution (NaOH), (b) alkali treatment by sodium chlorite solution ($NaClO_2$), (c) alkali treatment by NaOH solution and surface treatment by ureidosilane coupling agent (3-ureidopropyltrimethoxy silane, A-1160) (NaOH + ureidosilane), and (d) alkali treatment by $NaClO_2$ solution and surface treatment by ureidosilane ($NaClO_2$ + ureidosilane) were used for the surface treatment of hemp fiber in this study.

3.2. Materials and methods

The materials used in this study were various surface-treated hemp fiber-reinforced plant-derived polyamide 1010 biomass composites (HF/PA1010). PA1010, which is made from plant-derived castor oil, was used as the matrix polymer. Hemp fiber (HF, ϕ50–100 μm) was used as the reinforcement fiber. These materials are described in detail in the previous section 2. The volume fraction of fiber V_f was fixed with 20 vol.%. Hemp fibers were precut into 5-mm-long pieces and surface-treated by four types of surface treatments: (a) alkali treatment by sodium hydroxide solution (NaOH), (b) alkali treatment by sodium chlorite solution ($NaClO_2$), (c) alkali treatment by NaOH solution and surface treatment by ureidosilane coupling agent (S3, 3-ureidopropyltrimethoxy silane, A-1160, Momentive Performance Material Inc., USA) (NaOH + ureidosilane), and (d) alkali treatment by $NaClO_2$ solution and surface treatment by ureidosilane ($NaClO_2$ + ureidosilane). Two types of alkali treatment aqueous solutions such as sodium hydroxide solution (by NaOH) or and sodium chlorite solution ($NaClO_2$) were used as the mercerization agent. Alkali treatment by NaOH and $NaClO_2$ was employed as follows: 5% alkali agent solution was placed in a stainless beaker. Then chopped hemp fibers were added into the beaker and stirred well. This was kept at room temperature for 4 h. The fibers were then washed thoroughly with water to remove the excess of alkali agents sticking to the fibers. The alkali-treated fibers were dried in air for 12 h and in a vacuum oven at 80°C for 5 h. The surface treatment of hemp fibers with the concentration of 1 wt.% ureidosilane coupling agent (S3) was carried out in 0.5 wt.% acetic acid aqueous solution in which the pH of the solution was adjusted to 3.5 and stirred continuously for 15 min. Then, the fibers were immersed in the solution for 60 min. The surface-treated hemp fibers (HF-S) were removed from the solution and kept in air for 12 h and in a vacuum oven at 80°C for 5 h. All the components were dried for 12 h at 80°C in a vacuum oven beforehand until the moisture level was below 0.2%, and then dry blended in a small bottle, and subsequently the melt was mixed at 85 rpm and 220°C on a twin screw extruder (TEX-30, Japan Steel Works, Ltd., Japan). After mixing, the extruded strands of various HF/PA1010 biomass composites were cut in piece of about 5-mm long by the pelletizer, and dried again at 24 h at 80°C in a vacuum oven. In addition, 1-mm-thick sheets were compression-molded at the conditions of

http://dx.doi.org/10.5772/64215

220°C, 5 MPa, and 3 min, and cut into ϕ25-mm-disk shapes for rheological property measurements. The rheological properties in the molten state were evaluated by oscillatory flow testing using a parallel plate-type rotational rheometer (ARES, Rheometrix Scientific Co., USA). The diameter of the parallel plate was ϕ25 mm, and the gap between the two plates was fixed at 1 mm. Under such a gap condition, the test specimens were slightly compressed in the molten state. The angular frequency was varied from 10^{-1} to 10^{2} rad/s, and the strain amplitude was set as 1%. These measurements were carried out at 200–240°C. The dynamic viscoelastic properties in the molten state were evaluated by storage modulus G', loss modulus G'', loss tangent tan δ, phase angle δ (=arctan G''/G'), complex modulus $|G^*|$, and complex viscosity $|\eta^*|$. The surface of fiber and the composites fractured cryogenically in liquid nitrogen were observed using a scanning electron microscope (SEM, JSM-6360LA, JEOL Ltd., Japan). Fiber surface roughness such as arithmetic mean estimation R_a was measured using a laser microscope (VK-X200, Keyence Co., Japan). Fourier transform infrared spectroscopy (FT-IR) measurements were performed by a FT-IR spectrometer (FT/IR-6100, JASCO Co., Japan) using the attenuated total reflection (ATR) technique by a diamond prism. A total of 64 scans were taken for each sample between 400 and 4000 cm^{-1}, with a resolution of 8 cm^{-1}.

3.3. Angular frequency dependences

The dynamic viscoelastic properties of various surface-treated hemp fiber-filled plant-derived polyamide 1010 biomass composites (HF/PA1010) in molten state were evaluated by oscillatory behavior. The dynamic viscoelastic properties in the molten state are strongly dependent on the internal microstructure of the polymer composites. We shall discuss the angular frequency dependences, which is the basic variable in dynamic viscoelastic properties. **Figure 4(a)** shows the effects of alkali treatment on the relationship between storage modulus G' and angular frequency ω of various HF/PA1010 biomass composites at 220°C. G' of neat PA1010 (100%) increases with increasing ω, in agreement with the linear dynamic viscoelastic model that G' is proportional to ω^2 (log $G' \propto 2\log \omega$) [31, 32]. G' of various HF/PA1010 biomass composites shows the typical storage modulus G' of highly filled systems (such as gel systems), indicating the "second rubbery plateau," i.e., the long-scale relaxation time [21, 31–35]. This

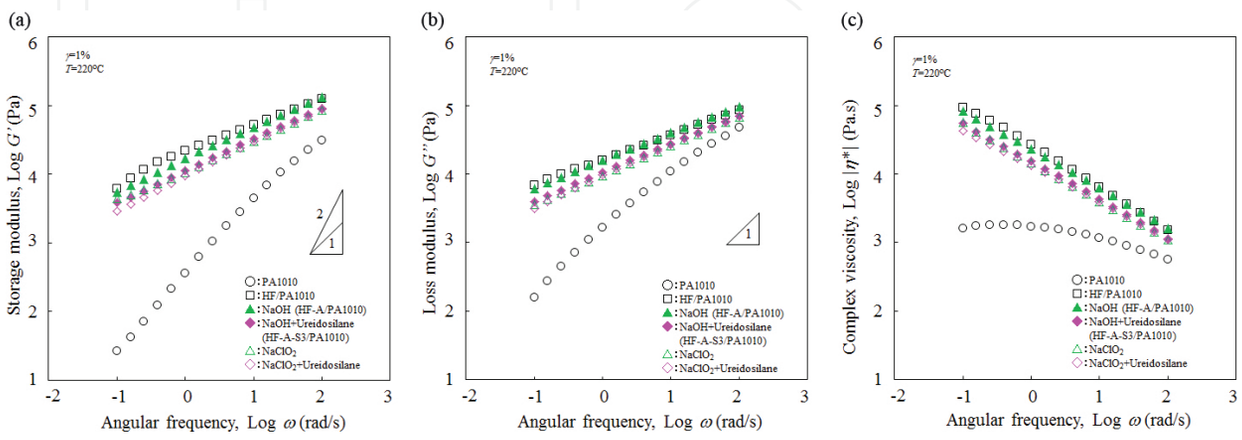

Figure 4. Dynamic viscoelastic properties as a function of angular frequency for various HF/PA1010 biomass composites. (a) Storage modulus, (b) loss modulus, and (c) complex viscosity.

behavior may be attributed to the internal structure formation such as fiber network formation, which is due to high aspect ratio of HF and the interfacial interaction between HF and PA1010. However, the slope of G' against ω of various HF/PA1010 biomass composites in low w region changes with the type of alkali treatment and decreases in the following: Untreated > NaOH > $NaClO_2$ > NaOH + ureidosilane (S3) > $NaClO_2$ + ureidosilane (S3). **Figure 4(b)** shows the effect of alkali treatment on the relationship between loss modulus G'' and ω. G'' of neat PA1010 monotonically increases with an increasing ω in the whole range of ω. This is in agreement with the linear viscoelastic model that the slope of G'' is proportional to ω ($\log G'' \propto \log \omega$). On the contrary, various HF/PA1010 biomass composites show different tendencies and the slope of G'' against w becomes small in the low w region. However, this tendency of G'' is smaller than that of G' since G' is a more sensitive viscoelastic function with respect to the structural changes of the composites compared G'' [36–38]. **Figure 4(c)** shows that the effect of alkali treatment on the relationship between the complex viscosity $|\eta^*|$ and ω. $|\eta^*|$ of neat PA1010 does not change with ω in the low ω regions, which demonstrates Newtonian behavior, and this slightly decreases with increasing ω in the high w region. On the contrary, the effect of various HF/PA1010 biomass composites rapidly decreases with increasing ω in a wide range and in magnitude orders more viscous than neat PA1010 even at high ω regions. Various HF/PA1010 biomass composites exhibit very strong shear-thinning effect, ant the curves of $|\eta^*|$ vs. ω have a slope of −45°. This behavior indicates the presence of an apparent yield stress in the low ω regions.

3.4. Effect of alkali treatment

In general, dynamic viscoelastic properties such as storage modulus G' are considered to be sensitive indicators for the quantitative analysis of morphological changes in the polymer composites as mentioned earlier. To clarify the effect of alkali treatment on the dynamic viscoelastic properties of the HF/PA1010 biomass composites, the relative storage modulus G'_r of various alkali-treated HF/PA1010 biomass composites in the low ω region (ω=0.25 rad/s) is shown in **Figure 5**. Here, the relative storage modulus is given by the values of surface-treated HF/PA1010 composites divided by that of untreated ones. The values of G'_r decrease in the following order: NaOH > $NaClO_2$ > NaOH + ureidosilane (S3) > $NaClO_2$ + ureidosilane (S3). The important findings in this results are (1) the elastic properties such as the storage modulus decreases with surface treatment by alkali and silane coupling agent, (2) the reducing ratio of G'_r of $NaClO_2$ is higher than that of NaOH, and (3) the combination of $NaClO_2$ + ureidosilane (S3) has the strongest effect on G'_r among all surface treatments in this study. The possible reasons of these phenomena are onset of self-lubrication of HF, three-dimensionally oriented fiber structure formation which may reduce the storage modulus of the surface-treated HF/PA1010 biomass composites to less than that of the untreated systems, and different roles played by the alkali treatment and silane coupling agent during the processing. It is, however, difficult to establish the exact reasons in the present stage.

http://dx.doi.org/10.5772/64215

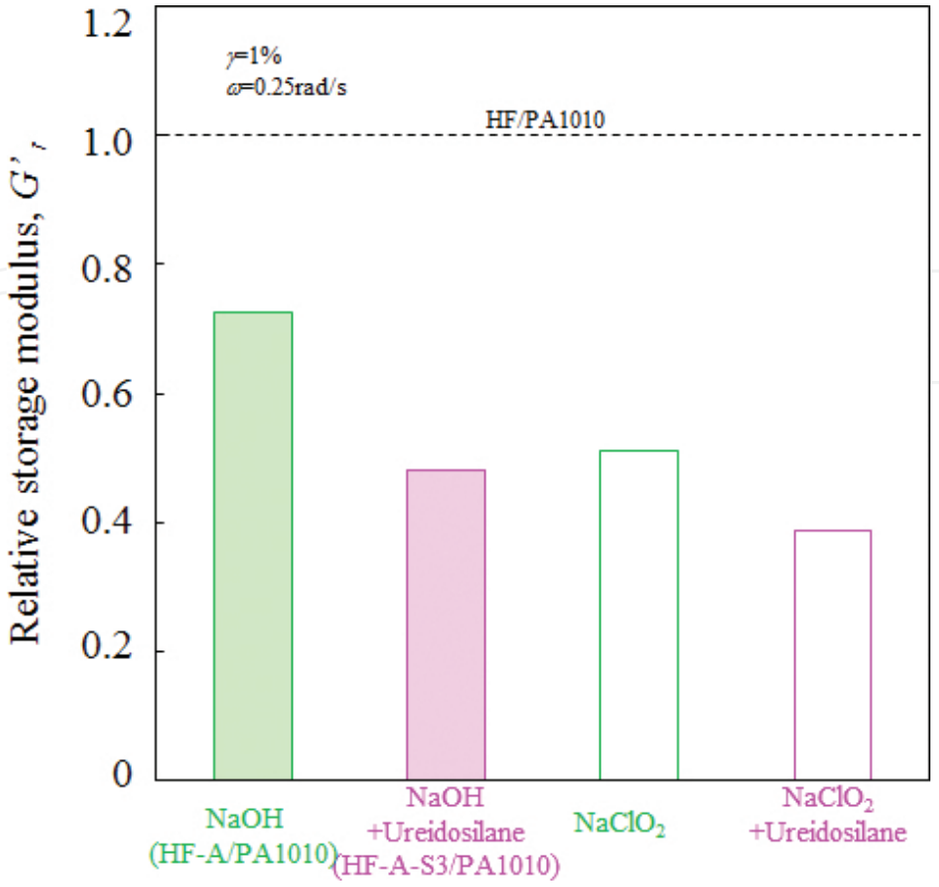

Figure 5. The relative storage modulus for various HF/PA1010 biomass composites.

3.5. Morphology and chemical analysis

To further clarify the relationship between the dynamic viscoelastic properties and internal structure formation of HF/PA1010 composites, we discuss the morphologies of these composites, which are internal structure formation such as fiber network formation and the interfacial interaction between HF and PA1010. **Figure 6** shows the SEM observation results of the HF surface before/after the alkali treatment. The surface roughness of HF increases with alkali treatment. The results of measuring the average surface roughness (arithmetic average roughness R_a) using a laser microscope are R_a = 3.2 mm (untreated), R_a= 3.4 mm (NaOH), and R_a =5.1 mm ($NaclO_2$), respectively. In particular, $NaClO_2$ treatment increases bumps and surface roughness significantly. These measurement results indicate that the attackability of HF differs according to the type of alkaline coupling agent. It is well known that alkali treatment promotes the disruption of hydrogen bonding in the network structure of natural fiber and removes the lignin and hemicellulose [4, 22]. Therefore, this treatment increases not only the surface roughness resulting in better unlocking but also the amount of cellulose exposed on the fiber surface, thereby increasing the number of possible reaction sites. Consequently, the interfacial interaction between fiber (HF) and matrix polymer (PA1010) (or silane coupling agent) also increases.

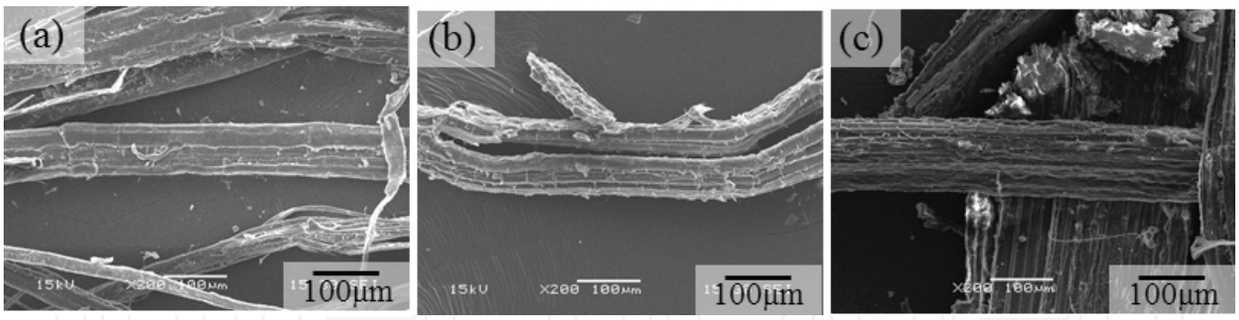

Figure 6. SEM photographs of untreated and alkali-treated hemp fibers. (a) Untreated: R_a= 3.2 mm, (b) NaOH (HF-A): R_a= 3.4 mm, and (c) $NaClO_2$: R_a= 5.1 mm.

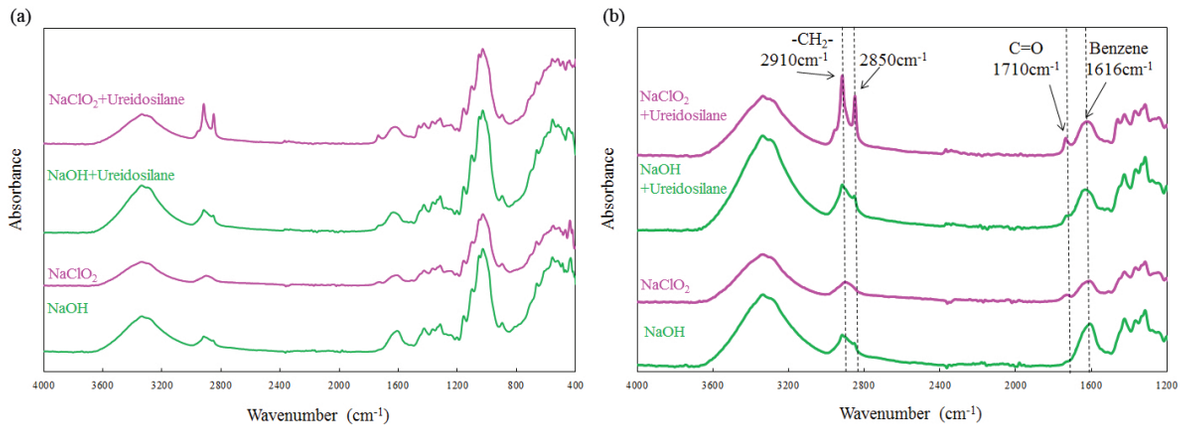

Figure 7. FT-IR spectra of various surface treated hemp fibers. (a) 400–4000 cm^{-1} and (b) 1200–4000 cm^{-1}.

It is essential to investigate chemical analyses such as Fourier transform infrared spectroscopy (FT-IR) in order to determine the chemical composition of the fiber surface. There have been various investigations on the effect of various surface treatments on the characterization of natural fiber surface [22, 26, 39, 40]. We shall discuss the observation of the characterization of the fiber surface using FT-IR. **Figure 7** shows the FT-IR spectra of various alkali-treated HFs: 400–4000 cm^{-1} (**Figure 7(a)**) and 1200–4000 cm^{-1} (**Figure 7(b)**). In the case of different alkali treatments such as NaOH and $NaClO_2$, the reduction of some vibrations, which are 1400–1500 cm^{-1} region associated with CH_2 bending of pectin, lignin, and hemicellulose, 1616 cm^{-1} related with benzene ring stretching of lignin, 2850–2910 cm^{-1} region associated with CH_2 stretching of Wax and C-H stretching of polysaccharides, and 3200–3600 cm^{-1} region corresponded with OH stretching of polysaccharides, is observed [22, 26, 39]. In particular, the peak at 1710 cm^{-1} is attributed to the C=O stretching of the acetyl groups of hemicellulose [26, 39]. The removal of hemicellulose from the fiber surfaces causes the peak to disappear [22, 26]. On the contrary, the FT-IR spectra of surface treatment by ureidosilane (S3) present some clear peaks, which are 1710 cm^{-1} corresponding with C=O stretching, 2850 and 2910 cm^{-1} related with CH_2 stretching, and 3200–3600 cm^{-1} region associated with OH stretching. These findings indicate the following: alkali treatment by $NaClO_2$ has more attackability on HF than that by NaOH.

http://dx.doi.org/10.5772/64215

Accordingly, the former is able to completely remove lignin, wax, and hemicellulose from hemp fiber bundles and replaces more OH groups the hemp fiber surfaces. Meanwhile, the peaks at 1710, 2850, and 2910 cm^{-1} show the presence of silane in the surface treatment by ureidosilane (S3), although the same peak is not present in the only alkali treatment. This may be attributed to the evidence of chemical bond between fiber and the silane coupling agent. Incidentally, Khan [41] and Sgriccia [39] have reported the presence of silane in fiber, which is the peak at 766 and 847 cm^{-1}. However, the concentration of silane on the fiber surfaces is too small to be detected by FT-IR in this study.

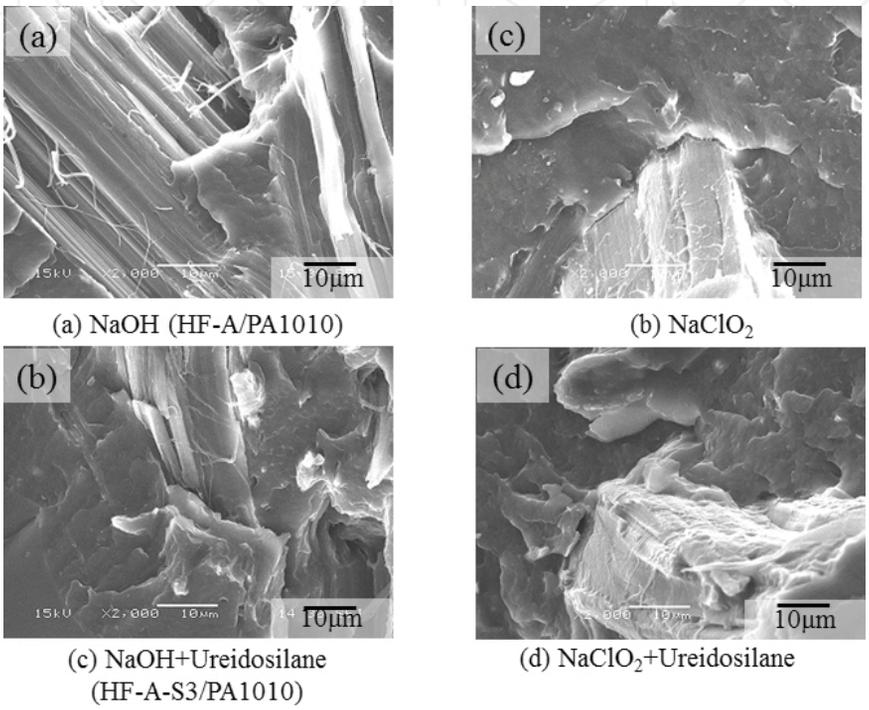

Figure 8. SEM photographs of cryogenically fractured surface of various HF/PA1010 biomass composites.

Furthermore, to clarify the interfacial interaction between fiber (HF) and matrix polymer (PA1010), we performed SEM observation of the fractured surface cryogenically in liquid nitrogen. **Figure 8** shows SEM photographs of cryogenically fractured surface of various HF/PA1010 biomass composites: (a) NaOH, (b) $NaClO_2$, (c) NaOH + ureidosilane (S3), and (d) $NaClO_2$ + ureidosilane (S3). The results of the comparison of the results in **Figure 8** suggest that the alkali treatment by $NaClO_2$ shows larger physical contact area between HF and PA1010 than that of NaOH. The morphologies of the composites surface-treated by NaOH (**Figure 8(a)**) and $NaClO_2$ (**Figure 8(b)**) show poor interaction between HF and PA1010. This indicates poor chemical contact between fiber and matrix polymer. On the contrary, the morphologies of the composites surface-treated by both alkali treatment and silane coupling agent (**Figure 8(c)** and **(d)**) show good interaction between fiber and matrix polymer, and fiber does not leave any voids on the fracture surface. This is attributed to the chemical reaction between the ureido group in the silane coupling agent and the possible reaction site on the fiber by $NaClO_2$ alkali treatment. These results are attributed to the good combination between $NaClO_2$ and ureido-

silane coupling agent (S3) for improving the rheological properties of HF/PA1010 biomass composites. These SEM image observations are in agreement with the mechanical properties such as tensile and bending results in previous report [16].

3.6. Temperature dependence

The effects of temperature on the viscoelastic properties of various surface-treated HF/PA1010 biomass composites are discussed here. The complex viscosity $|\eta^*|$ of various HF/PA1010 biomass composites is plotted against the reciprocal of the absolute temperature $1/T$ at the angular frequency ω of 25 rad/s in **Figure 9**. $|\eta^*|$ of all surface-treated HF/PA1010 biomass composites except for the NaOH systems is lower than that of the untreated ones. The effect of alkali treatment on $|\eta^*|$ of HF/PA1010 biomass composites differs for each surface treatment. In particular, NaOH + ureidosilane (S3) is most sensitive to temperature, while the untreated composites are the least. From the slope of $|\eta^*|$ vs. $1/T$ plots, the apparent activation energy E_α for flow can be calculated from the following Andrade's equation:

$$\eta = A\exp\left(\frac{E_a}{RT}\right) \tag{1}$$

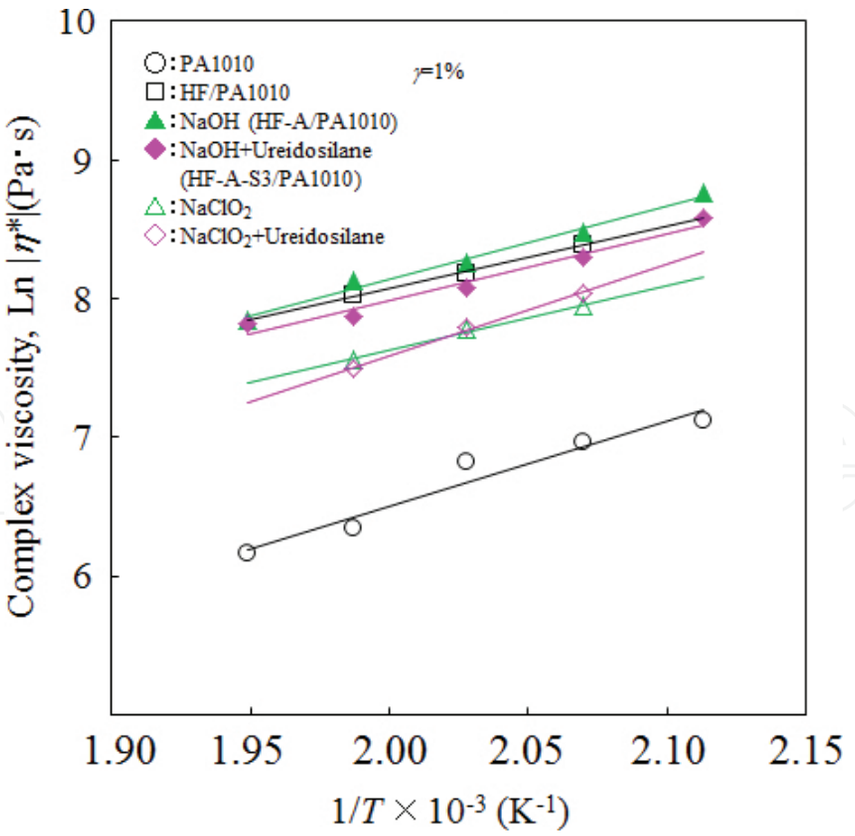

Figure 9. Temperature dependence of complex viscosity for various HF/PA1010 biomass composites.

http://dx.doi.org/10.5772/64215

where A is the constant value, R is the gas constant, and η was replaced by $|\eta^*|$ [12, 33]. The apparent activation energy E_a of various HF/PA1010 biomass composites is listed in **Table 2**. It was found that E_a increases in the following order: untreated (HF) < $NaClO_2$ < NaOH + ureidosilane (S3) < NaOH < pure PA1010 < $NaClO_2$ + ureidosilane (S3). It can be said that the fluidity of the materials increases with increasing Ea. Briefly, $NaClO_2$ + ureidosilane (S3) with the highest value of E_a indicates high sensitivity to temperature changes.

Code	PA1010	HF/PA1010	NaOH (HF-A/PA1010)	NaOH+ Ureidosilane (HF-A-S3/PA1010)	$NaClO_2$	$NaClO_2$+Ureidosilane
E_a (kJ/mol)	50.5	37.4	44.2	39.9	38.3	55.1

Table 2. The apparent activation energy of various HF/PA1010 biomass composites.

4. Influence of type of silane coupling agent on dynamic viscoelastic properties of hemp fiber-reinforced plant-derived polyamide 1010 biomass composites in the molten state

4.1. Introduction

It is important to analyze the flow/deformation behavior of high-performance natural fiber-reinforced polymer biomass composites during the polymer processing and to investigate the flow mechanisms and changes in the internal structure of these biomass composites. In particular, although these biomass composites undergo various flow processes, the effect of surface treatment on the rheological properties has not been studied enough [12, 21, 34, 42–44]. Therefore, there is a need for proper rheological studies on the effect of surface treatment taking into account various factors such as type of fiber, size and size distribution, degree of agglomeration, and type of surface treatment. However, the determination of the effect of surface treatment on the interface or interphase adhesion between fiber and matrix polymer is thought to be a complicated task since these factors are interrelated. We reported the effect of alkali treatment on the dynamic viscoelastic properties of hemp fiber-reinforced plant-derived polyamide 1010 biomass composites in the molten state in the preceding section. According to our survey on the previous results, the influence of the type of silane coupling agent used on the rheological properties of these biomass composites is still not well known [12]. It is therefore necessary to systematically investigate it for the further understanding of this problem. This section reports the effects of the type of silane coupling agent used on the rheological properties, which are dynamic viscoelastic properties in the molten state, investigated experimentally, for hemp fiber-reinforced plant-derived polyamide 1010 biomass composites as mentioned earlier. It discusses the dynamic viscoelastic properties in terms of various factors: angular frequency, volume fraction, various kinds of silane coupling agents, and temperature.

4.2. Materials and methods

The materials used in this study were various surface-treated hemp fiber-filled polyamide 1010 biomass composites. Since the materials, processing, and experimental methods are similar to those mentioned in Section 3.2 other than the surface treatment by silane coupling agents, details are omitted here. Hemp fibers were previously cut into 5-mm-long pieces and surface-treated by two types of surface treatment: a) alkali treatment by sodium hydroxide (NaOH) solution and b) surface treatment by silane coupling agents. Alkali treatment by NaOH was employed as follows: 5% NaOH solution was placed in a stainless beaker. Then chopped hemp fibers were then added in the beaker and stirred well. This was kept at room temperature for 4 h. The fibers were then washed thoroughly with water to remove the excess NaOH sticking to the fibers. The alkali-treated fibers (HF-A) were dried in air for 12 h and in a vacuum oven at 80 °C for 5 h. Three types of silane coupling agents such as aminosilane (S1, 3-(2-aminoethylamino) propyltrimethoxy silane, A-1120, Momentive Performance Materials Inc., USA), epoxysilane (S2, 3-glycidoxypropyltrimethoxy silane, A-187), and ureidosilane (S3, 3-ureidopropyltrimethoxy silane, A-1160) were used as the surface treatment agents. The treatment of hemp fibers with the concentration of 1 wt.% of the chosen silane coupling agent was carried out in deionized water (for S1) or 5 wt.% acetic acid aqueous solution (for S2 and S3, where pH of the solution was adjusted to 3.5) and stirred continuously for 15 min. Then, the fibers were immersed in the solution for 60 min. After treatment, fibers were removed from the solution and dried in air for 12 h and in vacuum oven at 80°C for 5 h. The volume fraction of fiber V_f was varied with 10 and 20 vol.%/ The materials used in this section are listed in **Table 3**.

Code	Alkali treatment	Silane coupling agent
HF-A	NaOH	–
HF-A-S1	NaOH	Aminosilane (S1)
HF-A-S2	NaOH	Epoxysilane (S2)
HF-A-S3	NaOH	Ureidosilane (S3)

Table 3. Code, alkali treatment and silane coupling agent used in this study.

4.3. Angular frequency dependences

The rheological properties of various surface-treated hemp fiber-filled polyamide 1010 biomass composites (HF/PA1010) in molten state were evaluated by oscillatory flow behavior. The dynamic viscoelastic properties of various surface-treated HF/PA1010 biomass composites (HF content is 20 vol.%) are plotted as a function of angular frequency ω in **Figure 10(a)** (storage modulus G') and **Figure 10(b)** (loss modulus G''), respectively. The G' of various surface-treated HF/PA1010 biomass composites shows the typical storage modulus G' of highly filled systems, indicating the "second rubbery plateau" [21, 31–35]; however, the value of G' changes with the types of silane coupling agents used. The G' of aminosilane (HF-A-S1/PA1010) and epoxysilane (HF-A-S2/PA1010) is lower than that of untreated (HF/PA1010) in

http://dx.doi.org/10.5772/64215

wide ω regions. On the contrary, G' of ureidosilane (HF-A-S3/PA1010)-treated composites is at the same level of that of the untreated one in the low ω regions, although this is lower than that of untreated in the high ω regions. The slope of G' in the low ω region decreases in the following order: NaOH (HF-A) < ureidosilane (HF-A-S3) < epoxysilane (HF-A-S2) < aminosilane (HF-A-S1). This may be attributed to the change of interfacial interaction between HF and PA1010 according to the type of silane coupling agent used. These behaviors differ from the dynamic viscoelastic properties of the polymer composites such as glass fiber-reinforced polypropylene composites (GF/PP), in which G' of the surface-treated GF/PP by silane coupling agent is higher than that of untreated [21]. In general, the influence of surface treatment by coupling agents on the dynamic viscoelastic properties of the polymer composites is complex. This is because the surface treatment by coupling agents plays multiple roles simultaneously, coupling agent which improves the adhesion between the fiber and the polymer, lubricant which reduces friction, plasticizer which helps soften fiber and polymer, wetting agent which reduces the agglomeration of fibers, and additive for deforming fiber assembly easily and lowering the viscoelastic properties of the matrix polymer [21]. It is thought that the mechanisms mentioned earlier do not occur separately, and therefore it is very difficult to distinguish the factors of the coupling agent influencing the viscoelastic properties. On the contrary, loss modulus G'' of various surface-treated HF/PA1010 biomass composites is higher than that of pure PA1010; however, the effect of surface treatment by silane coupling agent on G'' of HF/PA1010 biomass composites does not differ according to the type of silane coupling agent used. This is because G' is a more sensitive rheological function to the structural changes of the internal structure of polymer composites compared to G''. In other words, G' is considered to be a sensitive indicator for the quantitative analysis of morphological changes in the composites as mentioned earlier. Next, the complex viscosity $|\eta^*|$ of various surface-treated HF/PA1010 biomass composites (HF content is 20 vol.%) is plotted as a function of angular frequency ω in **Figure 10(c)**. The $|\eta^*|$ of neat PA1010 does not change with ω in low ω region, which shows Newtonian behavior, and this slightly decreases with increasing ω in the high ω regions. On the contrary, the $|\eta^*|$of various HF/PA1010 biomass composites rapidly decreases with increasing ω in a wide range. The order of magnitude is more viscous than neat PA1010 even in the high ω regions. In addition, it is

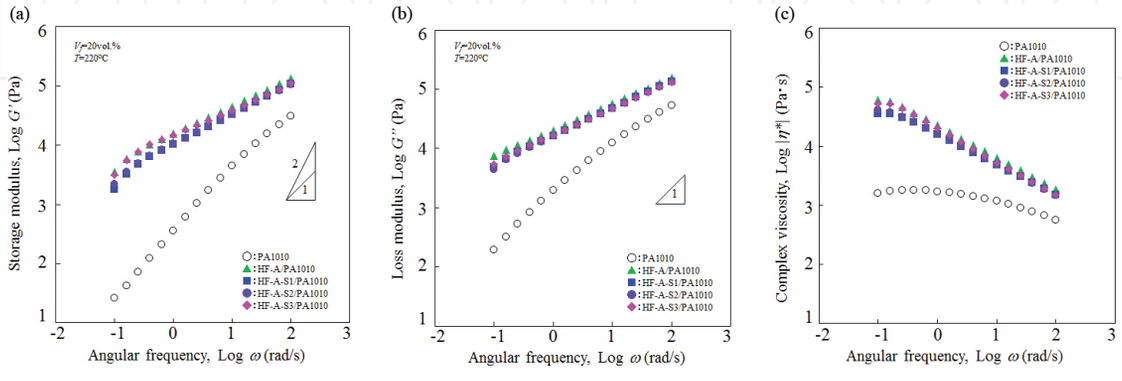

Figure 10. Dynamic viscoelastic properties as a function of angular frequency for various HF/PA1010 biomass composites. (a) Storage modulus, (b) loss modulus, and (c) complex viscosity.

interesting to note that the $|\eta^*|$ of all surface-treated HF/PA1010 composites by silane coupling agent shows a smaller value than NaOH-treated composites (HF-A/PA1010 composites).

4.4. Influence of volume fraction

The influence of volume fraction of fiber V_f on the rheological properties of various surface-treated HF/PA1010 biomass composites is discussed in this section. The relative complex viscosity $|\eta^*|_{r0}$ is plotted against volume fraction of fiber in **Figure 11**. Here, this relative value is given by the value of various surface-treated HF/PA1010 biomass composites divided by that of neat PA1010. The $|\eta^*|_{r0}$ of various surface-treated HF/PA1010 biomass composites increases with an increasing volume fraction of fiber V_f. This tendency changes with the type of silane coupling agent used. However, it is remarkably influenced by the volume fraction of fiber V_f rather than its types. These results may be attributed to the internal microstructure formed by the interaction between fibers rather than the interaction between fiber and matrix polymer. In addition, it was also found that aminosilane (HF-A-S1) is the least viscous of all silane coupling agents in this study. This behavior will be discussed in the next section.

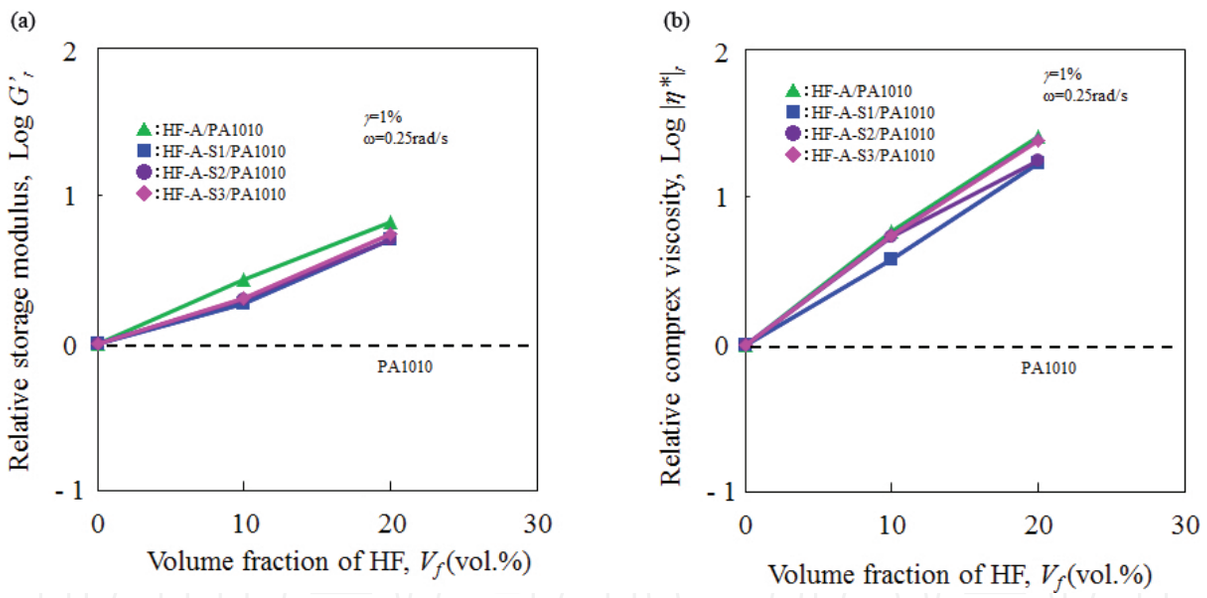

Figure 11. Influence of volume fraction of fiber on the dynamic viscoelastic properties of various HF/PA1010 biomass composites. (a) Relative storage viscosity and (b) relative complex viscosity.

4.5. Influence of type of silane coupling agent

To further clarify the effects of surface treatment by silane coupling agent on the rheological properties of HF/PA1010 biomass composites, the relative storage modulus G'_r of various surface-treated HF/PA1010 biomass composites is shown in **Figure 12(a)** (ω=0.25 rad/s) and **Figure 12(b)** (ω=25 rad/s), respectively. Here, the relative storage modulus is given by the values of surface-treated HF/PA1010 composites divided by those of NaOH-treated ones (HF-A/PA1010 composites). The values of G'_r in the low ω regions (ω = 0.25 rad/s) differ accord-

http://dx.doi.org/10.5772/64215

ing to the type, and G'_r of aminosilane (HF-A-S1) and epoxysilane (HF-A-S2) remarkably decreases although that of ureidosilane (HF-A-S3) is almost the same as that of the NaOH-treated composites. Contrarily, the G'_r of all HF/PA1010 composites in the high ω regions (ω = 25 rad/s) is lower than that of the NaOH-treated ones and slightly decreases in the following order: ureidosilane (HF-A-S3) > epoxysilane (HF-A-S2) > aminosilane (HF-A-S1). Thus, the effect of the type of silane coupling agent used on the storage modulus of HF/PA1010 biomass composites changes with the difference in the frequency region. It is well known that the storage modulus in the low ω region is influenced by the strong interaction of fiber–matrix polymer and/or fiber–fiber and the microstructure formation by the fibers. On the contrary, this value in the high ω region is generally dominated by the matrix polymer. From the results shown above, it can be concluded that the various silane coupling agents decrease the storage modulus, and silane coupling agents used in this study play the role of the lubricant, the wetting agent, or the plasticizer, supported by the facts in **Figure 12(a)** and **(b)**. However, only ureidosilane (HF-A-S3) may play the vital role of the coupling agent which improves the interaction between fiber and matrix polymer as the G' values of ureidosilane (HF-A-S3) are higher than those of the other systems. This tendency was also observed for the mechanical and tribological properties of these biomass composites [10, 11, 16].The relative complex viscosity $|\eta^*|_r$ of various surface-treated HF/PA1010 biomass composites is shown in **Figure 12(c)** (ω=0.25 rad/s) and **Figure 12(d)** (ω=25 rad/s), respectively. Here, the relative complex viscosity is given by the values of surface-treated HF/PA1010 composites divided by that of the NaOH-treated ones (HF-A/PA1010 composites). $|\eta^*|_r$ has the same tendency as that for G'_r. Briefly, the viscoelastic properties of HF/PA1010 biomass composites decrease with surface treatments using the silane coupling agent and are highly influenced by angular frequency.

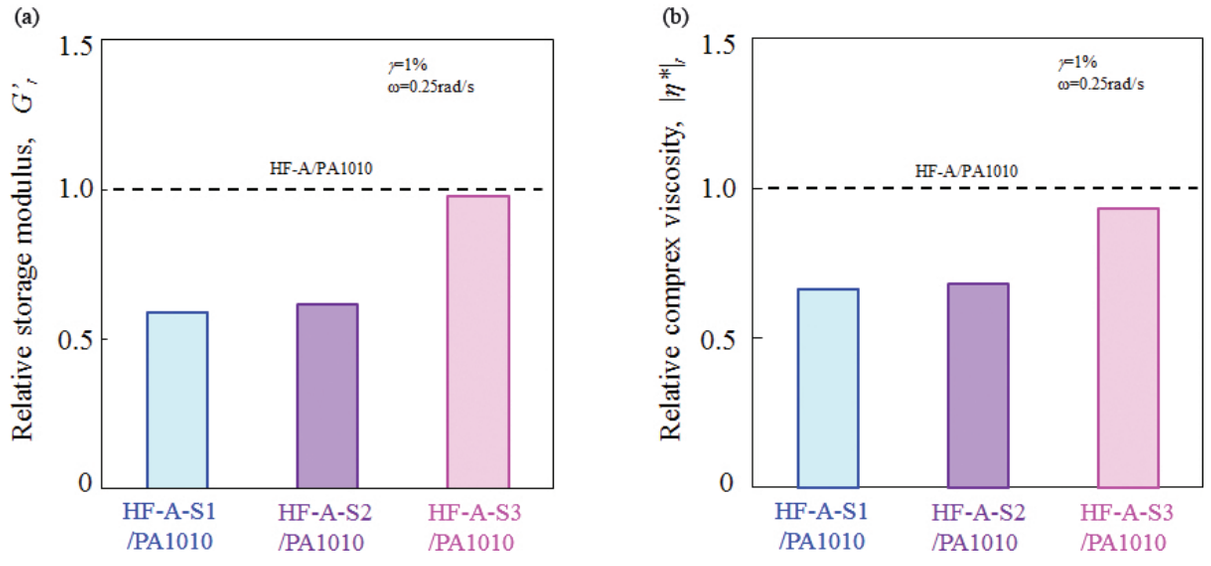

Figure 12. The relative values for various surface-treated HF/PA1010 biomass composites. (a) Relative storage modulus and (b) relative complex viscosity.

4.6. Temperature dependences

The influence of temperature on the viscoelastic properties of surface-treated HF/PA1010 biomass composites is discussed here. The complex viscosity $|\eta^*|$ of various surface-treated HF/PA1010 composites is plotted against the reciprocal value of the absolute temperature $1/T$ at the angular frequency ω of 25 rad/s in **Figure 13**. The $|\eta^*|$ of all surface-treated HF/PA1010 composites using silane coupling agent is lower than that of the NaOH-treated ones (HF-A/PA1010 composites), and the difference of the value increases with increasing temperature. The influence of temperature on $|\eta^*|$ of HF/PA1010 composites differs for each surface treatment using silane coupling agent. It is found that epoxysilane (HF-A-S2) is the most temperature sensitive, and ureidosilane (HF-A-S3) is the least. From the slope of $|\eta^*|$ vs. $1/T$ plots, the apparent activation energy E_a for flow can be calculated from the previous Andrade's equation (1). **Figure 14** shows the apparent activation energy E_a of various HF/PA1010 biomass composites. It was found that E_a increases in the following order: ureidosilane (HF-A-S3) < NaOH (HF-A) < aminosilane (HF-A-S1) < neat PA1010 < epoxysilane (HF-A-S2). It can be said that the fluidity of the materials increases with increasing E_a. Briefly, epoxysilane (HF-A-S2) with the highest value of E_a demonstrates high sensitivity to temperature changes. This means that ureidosilane (HF-A-S3) with the lowest value of E_a has stable flow processability in a wide temperature region for the HF/PA1010 biomass composites studied here.

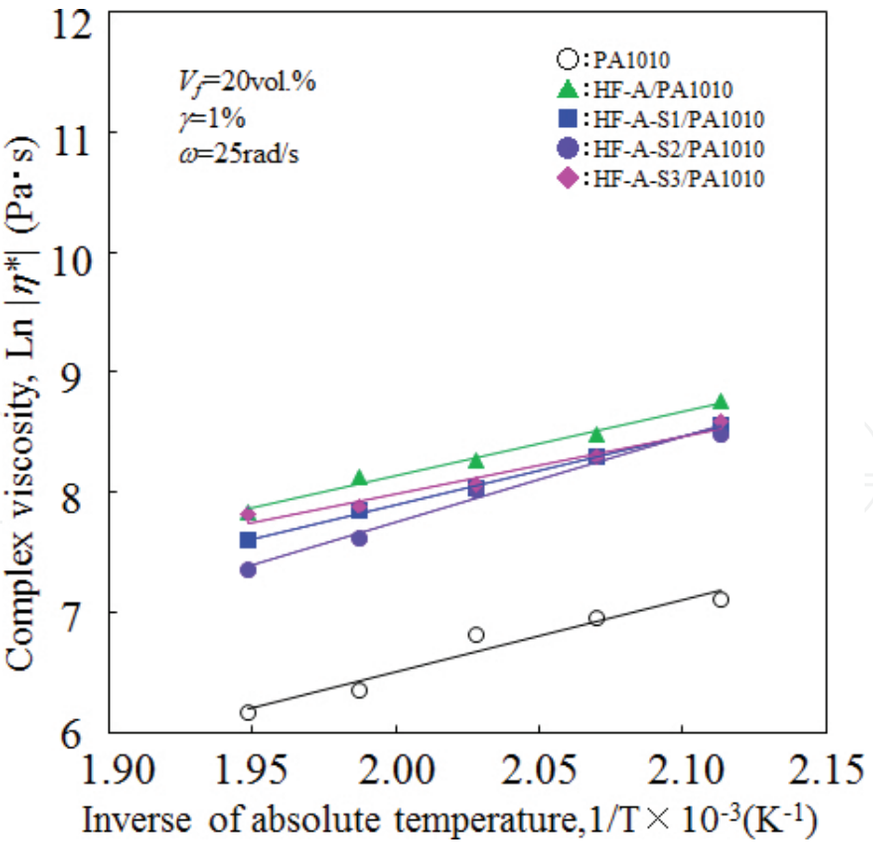

Figure 13. Temperature dependence of complex viscosity for various surface-treated HF/PA1010 biomass composites.

http://dx.doi.org/10.5772/64215

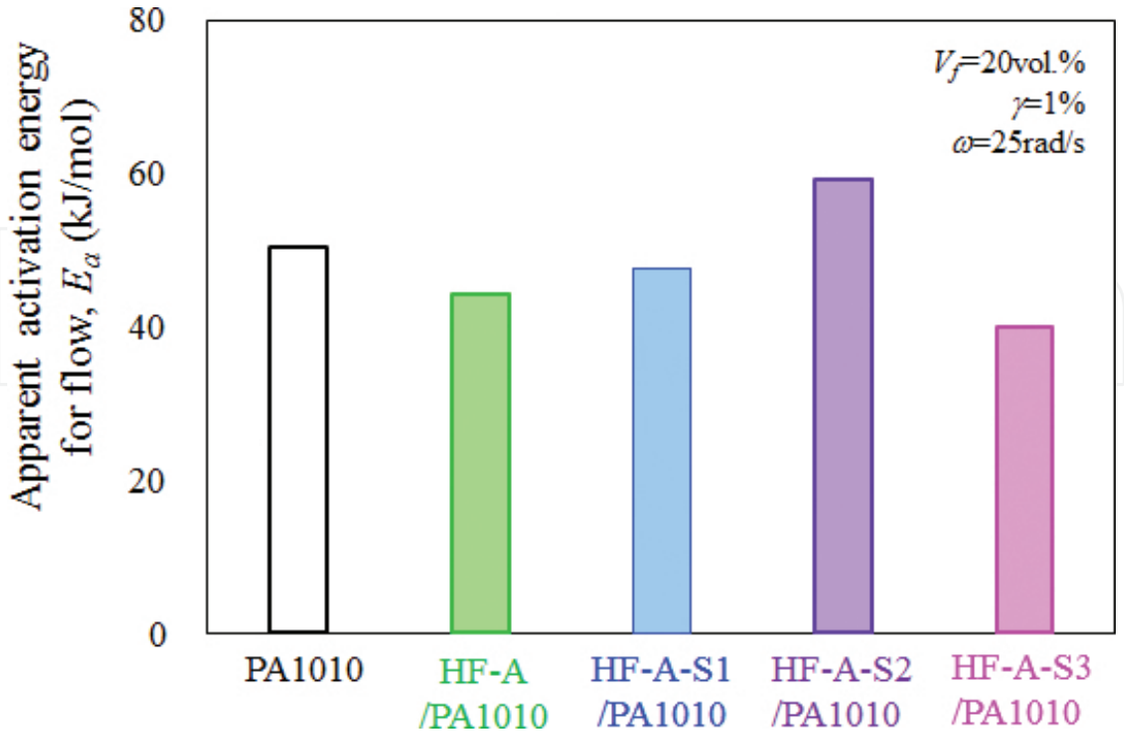

Figure 14. The apparent activation energy E_a of various HF/PA1010 biomass composites.

4.7. Complex modulus dependences

The complex modulus dependence of various surface-treated HF/PA1010 biomass composites in the molten state is discussed in this section. **Figure 15** shows the phase angle δ (=arctan G''/G') is plotted against the absolute value of the complex modulus $|G^*|$ of various surface-treated HF/PA1010 biomass composites. The van Gurp–Palmen plot [45] is drawing attention recently as another method for representing internal microstructures and their changes. This plot is considered to be a sensitive indicator for the time-temperature superposition, the presence of long chain branch of the polymer, gelation behavior, rheological percolation of polymer nanocomposites, etc. [45–47]. This is because the changes in the rheological properties, from which it is hard to understand the angular frequency dependence (G′- ω, G″- ω, tan δ – ω curves), are emphasized in this δ-$|G^*|$ plot. As seen in **Figure 15**, the δ-$|G^*|$ curve of neat PA1010 approaches 90° at the low complex modulus $|G^*|$, indicating the flow behavior of viscous fluid. On the contrary, the δ-$|G^*|$ curves of various surface-treated HF/PA1010 biomass composites show the complex behavior. However, these are of minimal value. In particular, ureidosilane (HF-A-S3), which is considered to play a strong role as a coupling agent for improving the interfacial interaction between the fiber and polymer, clearly shows the minimum value. It is also the lowest value compared to other surface treatment systems. On the contrary, the other composites which play a weak role as a coupling agent, do not show the minimum values. Thus, this δ-$|G^*|$ plot may be able to serve as an indicator for the effect of surface treatment of polymer composites.

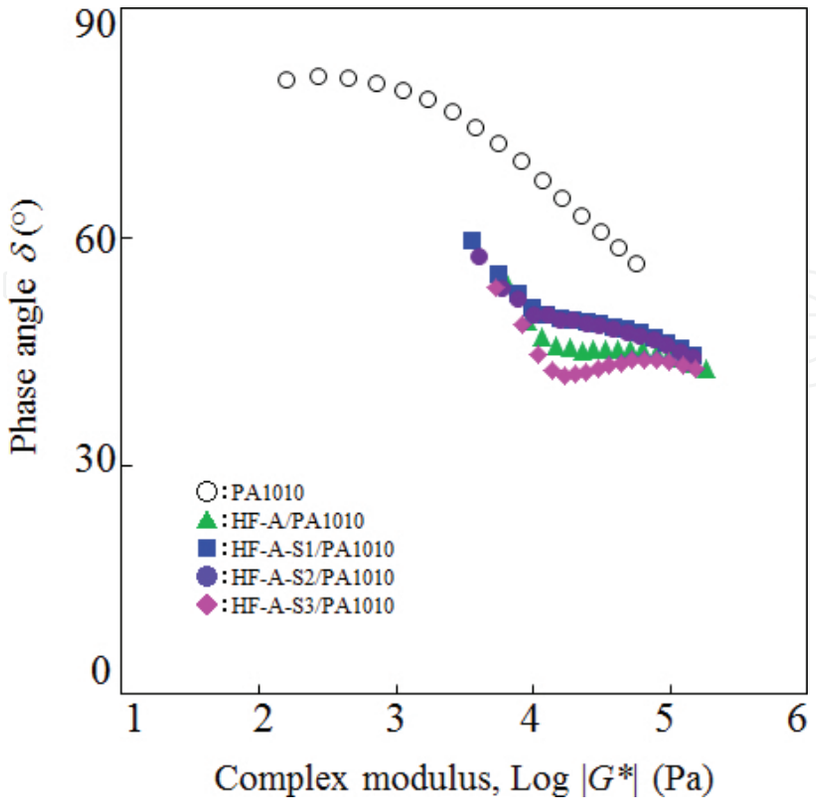

Figure 15. The phase angle is plotted against the absolute value of the complex modulus of various HF/PA1010 biomass composites.

5. Conclusion

The aim of this study is to investigate the thermal properties of hemp fiber-filled plant-derived polyamide 1010 biomass composites and their dynamic viscoelastic properties of these composites in the molten state experimentally. It was found that the addition of HF with PA1010 has a strong influence on the thermal properties such as DMA, TGA, and DSC. In particular, HF is effective for improving thermal and mechanical properties. The effect of alkali treatment on the dynamic viscoelastic properties of HF/PA1010 composites in the molten state differs according to whether the alkali treatment uses the silane coupling agent or not. In particular, the viscoelastic properties (both storage and loss moduli) of $NaClO_2$ are higher than those of NaOH. The silane coupling agents have a remarkable influence on (1) rheological properties such as storage modulus, loss modulus, loss tangent, and complex viscosity in low angular frequency regions in the molten state, (2) temperature dependence of rheological properties, and (3) relationship between phase angle and complex modulus (van Gurp–Palmen plots). These rheological behaviors were also strongly influenced by the type of silane coupling agents used. The viscoelastic properties (both storage and loss moduli) of aminosilane and epoxysilane treated composites were lower, which those of ureidosilane-treated ones were

higher than the moduli of only alkali-treated composites. Ureidosilane-treated composites were the least temperature sensitive in the surface treated composites investigated here.

Acknowledgements

This work was supported by JSPS KAKENHI Grant Number 16K06750 and 25420735. We would like to thank the Functional Microstructured Surfaces Research Center (FMS, MEXT, Japan) of Kogakuin University, the Project Research of Research Institute for Science and Technology of Kogakuin University and the Ogasawara Foundation for the Promotion of Science & Engineering for funding this study, and partial support by the national budget of Czech Republic within the framework of the Centre of Polymer Systems project (reg. number: CZ. 1.05/2.1.00/ 03.0111). The authors thank Mr. J. Mukaida, Ms. M. Hasumi, Mr. K. Nakamura and many master course and undergraduate course students at the Polymeric Materials Laboratory of Kogakuin University for their assistance with the experiments.

Author details

Yosuke Nishitani[1*], Toshiyuki Yamanaka[2], Tetsuto Kajiyama[3] and Takeshi Kitano[4]

*Address all correspondence to: at13152@ns.kogakuin.ac.jp

1 Department of Mechanical Engineering, Faculty of Engineering, Kogakuin University, Tokyo, Japan

2 Tokyo Metropolitan Industrial Technology Research Institute, Tokyo, Japan

3 Jonan Branch, Tokyo Metropolitan Industrial Technology Research Institute, Tokyo, Japan

4 Polymer Centre, Faculty of Technology, Tomas Bata University in Zlin, Zlin, Czech Republic

References

[1] Wibowo AC., Mohanty AC., Misra M., Lawrence T., Drzal LT. Chopped industrial hemp fiber reinforced cellulosic plastic biocomposites: Thermomechanical and morphological properties. Thermomechanical and morphological properties. Ind. Eng. Chem. Res. 2004;43:4883–4888. DOI: 10.1021/ie030873c

[2] Petersson L., Oksman K., Biopolymer based nanocomposites. Comparing layered silicates and microcrystalline cellulose as nanoreinforcement. Sci. Technol. 2006;66:2187–2196. DOI: 10.1016/j.compscitech.2005.12.010

[3] Bledzki AK., Gassan J., Composites reinforced with cellulose based fibres. Prog. Polym. Sci. 1999;24:221–274. DOI: 10.1016/S0079-6700(98)00018-5

[4] Omar F., Bledzki AK., Fink H-P., Sain M. Biocomposites reinforced with natural fibers: 2000–2010. Prog. Polym. Sci. 2012;37:1552–1596. DOI: 10.1016/j.progpolymsci. 2012.04.003

[5] John MJ., Thomas S. Biofibres and biocomposites. Carbohydrate Polymers. 2008;71:343–364. DOI: 10.1016/j.carbpol.2007.05.040

[6] Li X., Tabil L.G., Panigrahi S. Chemical treatments of natural fiber for use in natural fiber-reinforced composites: A review. J. Polym. Environ. 2007;15:25–33. DOI: 10.1007/s10924-006-0042-3

[7] Kalia S, Kaith B.S., Kaur I. Pretreatments of natural fibers and their application as reinforcing material in polymer composites – a review. Polym. Eng. Sci. 2009;49:1253–1272. DOI: 10.1002/pen.21328

[8] Xie Y., Hill CAS., Xiao Z., Militz H., Mai C. Silane coupling agents used for natural fiber/polymer composites: A review. Composites Part A. 2010;41:806–819. DOI: 10.1016/j.compositesa.2010.03.005

[9] Oksman K., Skrifvars M., J.-F. Selin. Natural fibres as reinforcement in polylactic acid (PLA) composites. Compos. Sci. Technol. 2003;63:1317–1324. DOI: 10.1016/S0266-3538(03)00103-9

[10] Hasumi M., Nishitani Y., Kitano T. Mechanical properties of hemp fiber filled polyamide 1010 composites. In: The Proceedings of Seikei-kako Symposia'11; 14–17 October 2011; Akita (in Japanese). 2011. p. 491–492.

[11] Hasumi M., Nishitani Y., Kitano T. Effect of surface treatment on the mechanical properties of hemp fiber reinforced polyamide 1010 composites. In: The Proceedings of the Polymer Processing Society 28th Annual Meeting (PPS-28); 11–15 December 2012; Pattaya. 2012. p. 07-324.

[12] Nishitani Y., Hasumi M., Kitano T. Influence of silane coupling agents on the rheological behavior of hemp fiber filled polyamide 1010 biomass composites in molten state. In: AIP Conference Proceedings; "Cleveland, Ohio, USA" 2015; 1664: 060007. Cleveland, Ohio, USA, http://dx.doi.org/10.1063/1.4918425

[13] Nishitani Y., Mukaida J., Yamanaka T., Kajiyama T., Kitano T.. Effect of processing sequence on the dynamic viscoelastic properties of ternary biomass composites (hemp fiber/ PA1010/ PA11E) in the Molten State. In: The Proceedings of Regional Conference of Polymer Processing Society (PPS-2105); 21–24 September 2015; Graz. 2015. Nat-81.

[14] Nishitani Y., Mukaida J., Yamanaka T., Kajiyama T., Kitano T. Thermal properties of hemp fiber filled polyamide 1010 biomass composites and the blend of these composites and polyamide 11 elastomer. In: The Proceedings of the 31st International Conference of the Polymer Processing Society (PPS-31); 7–11 June 2015; Jeju. 2015. p. 1116-1120.

[15] Mukaida J., Nishitani Y., Kitano T. Effect of addition of plants-derived polyamide 11 elastomer on the mechanical and tribological properties of hemp fiber reinforced polyamide 1010 composites, AIP Conference Proceedings "Cleveland, Ohio, USA" 2015; 1664: 060008. Cleveland, Ohio, USA, http://dx.doi.org/10.1063/1.4918426

[16] Mukaida J., Nishitani Y., Kajiyama T., Yamanaka T., Kitano T. Influence of types of alkali treatment on the mechanical properties of hemp fiber reinforced polyamide 1010 composites. In: The Proceedings of Regional Conference of Polymer Processing Society (PPS-2105); 21–24 September 201; Graz. 2015. Nat-104.

[17] Mukaida J., Nishitani Y., Kajiyama T., Yamanaka T., Kitano T. Effect of type of bio-TPE on the mechanical and tribological properties of plants-derived ternary composites (HF/PA1010/bio-TPE). J. Mater. Test. Res. Ass. Japan, 2016; 2016. p. 3–11.

[18] Naganuma M. Plants-derived polyamide "VESTAMID Terra" "VESTAMID HT Plus". JETI. 59; 2011. p. 88–90.

[19] Hausnerova B., Honkova N., Lengalova A., Kitano T., Saha P. Rheology and fiber degradation during shear flow of carbon-fiber-reinforced polypropylenes, Polym. Sci. Series A; 2006. p. 951–960. DOI: 10.1134/S0965545X06090100

[20] Hausnerova, B., Honkova, N., Lengalova, A., Kitano, T., Saha, P. Rheological behavior of fiber-filled polymer melts at low shear rate Part. I. Modeling of rheological properties. "Polimery/Polymers". (ISSN: 0032–2725). 2008;53:507–512.

[21] Nishitani Y., Ishii C., Kitano T. Rheological Properties of Surface Treated Glass Fiber Reinforced Polypropylenes in Molten State, Polypropylene, Dr. Fatih Dogan (Ed.), 2012. ISBN: 978-953-51-0636-4, InTech, Available from: http://www.intechopen.com/books/polypropylene/rheological-properties-ofsurface-treated-glass-fiber-reinforced-polypropylenes-in-molten-state

[22] Chand N, Fahim M. Tribology of Natural Fiber Polymer Composites. Woodhead Publishing Ltd; "Cambridge, England" 2008.

[23] Alawar A., Hamed AM., Al-Kaabi K. Characterization of treated date palm tree fiber as composite reinforcement. Compos. Part B Eng. 2009;40:601–606. DOI: 10.1016/j.compositesb.2009.04.018

[24] Aziz SH., Ansell MP. The effect of alkalization and fibre alignment on the mechanical and thermal properties of kenaf and hemp bast fibre composites: Part 1 – polyester resin matrix. Compos. Sci. Technol. 2004;64:1219–1230. DOI: 10.1016/j.compscitech.2003.10.001

[25] Abdelmouleh M., Boufi S., Belgacem M.N., Dufresne A. Short natural-fibre reinforced polyethylene and natural rubber composites: Effect of silane coupling agents and fibres loading. Compos. Sci. Technol. 2007;67:1627–1639. DOI: 10.1016/j.compscitech.2006.07.003

[26] Troedec ML., Sedan D., Peyratout C., Bonnet JP., Smith A., Guinebretiere R., Gloaguen V., Krausz P. Influence of various chemical treatments on the composition and structure of hemp fibres. Compos. Part A App. Sci. Manuf. 2008;39:514–522. DOI: 10.1016/j.compositesa.2007.12.001

[27] Araujo JR., Waldman WR., De Paoli MA. Thermal properties of high density polyethylene composites with natural fibres: Coupling agent effect. Polym. Degrad. Stab. 2008;93:1770–1775. DOI: 10.1016/j.polymdegradstab.2008.07.021

[28] Zeng H., Gao C., Wang Y., Watts PCP., Kong H., Cui X., Yan D. In situ polymerization approach to multiwalled carbon nanotube-reinforced nylon 1010 composites: Mechanical properties and crystallization behavior. Polymer. 2006;47:113–122. DOI: 10.1016/j.polymer.2005.11.009

[29] Li L., Li CY., Ni C., Rong L., Hsiao B. Structure and crystallization behavior of Nylon 66/multi-walled carbon nanotube nanocomposites at low carbon nanotube contents. Polymer. 2007;48:3542–3460. DOI: 10.1016/j.polymer.2007.04.030

[30] Choi JS., Lim ST., Choi HJ., Mohanty AK., Drzal LT., Misra M., Wibowo A. Preparation and characterization of plasticized cellulose acetate biocomposite with natural fiber. J. Mater. Sci. 2004;39:6631–6633. DOI: 10.1023/B:JMSC.0000044909.60878.97

[31] Ferry, JD. Viscoelastic Properties of Polymers. John Wiley & Sons, Incorporated; "New York, USA" 1980.

[32] Nishitani, Y., Yamada, Y., Ishii, C., Sekiguchi, I., Kitano, T. Effects of addition of functionalized sebs on rheological, mechanical, and tribological properties of polyamide 6 nanocomposites. Polym. Eng. Sci. 2010;50:100–112. DOI: 10.1002/pen.21516

[33] Nishitani, Y., Sekiguchi, I., Hausnerova, B., Nagatsuka, Y., Kitano, T. Dynamic viscoelastic properties of long organic fibre-reinforced polypropylene in molten state. Polym. Polym. Composi. 2001;9:199–211.

[34] Nishitani, Y., Sekiguchi, I., Hausnerova, B., Zdrazilova, N., Kitano, T. Rheological properties of aminosilane surface treated short glass fibre reinforced polypropylenes. Part 1: Steady shear and oscillatory flow properties in molten state. Polym. Polym. Composi. 2007;15:111–120.

[35] Nishitani, Y., Ohashi, K., Sekiguchi, I., Ishii, C., Kitano, T. Influence of addition of styrene-ethylene/butylene-styrene copolymer on rheological, mechanical, and tribological properties of polyamide nanocomposites. Polym. Composi. 2010;31:68–76. DOI: 10.1002/pc.20767

[36] Wan T., Clifford MJ., Gao F., Bailey AS., Gregory DH., Somsunan R. Strain amplitude response and the microstructure of PA/clay nanocomposites. Polymer. 2005;46:6429–6436. DOI: 10.1016/j.polymer.2005.04.105

[37] Durmus A., Kasgoz A., Macosko CW. Linear low density polyethylene (LLDPE)/clay nanocomposites. Part I: Structural characterization and quantifying clay dispersion by melt rheology. Polymer. 2007;48:4492–4502. DOI: 10.1016/j.polymer.2007.05.074

[38] Nishitani, Y., Sekiguchi, I., Ishii, C., Kitano, T. Dynamic viscoelastic properties of carbon nanofiber polyamide 66 composites in Molten State. Mater. Technol. 2010;28:135–145.

[39] Sgriccia N., Hawley MC., Misra M. Characterization of natural fiber surfaces and natural fiber composites. Compos. Part A. 2008;39:1632–1637. DOI: 10.1016/j.compositesa.2008.07.007

[40] Merlini C., Soldi V., Barra GMO. Influence of fiber surface treatment and length on physico-chemical properties of short random banana fiber-reinforced castor oil polyurethane composites. Polymer Test. 2011;30:833–840. DOI: 10.1016/j.polymertesting.2011.08.008

[41] Khan MA., Drzal LT. Characterization of 2-hydroxyethyl methacrylate (HEMA)-treated jute surface cured by UV radiation. J. Adhes. Sci. Technol. 2004;18:381–393. DOI: 10.1163/156856104773635481

[42] Shenoy AV. Rheology of Filled Polymer Systems. Kluwer Academic Publishers, Dordrecht, The Netherlands; 1999.

[43] Han CD., Van den Weghe T., Shete P., Haw JR. Effects of coupling agents on the rheological properties, processability, and mechanical properties of filled polypropylene. Polym. Eng. Sci. 1981;21:196–204.

[44] Khan SA., Prud'homme RK. Melt rheology of filled thermoplastics. Rev. Chem. Eng. 1987;4:205–272.

[45] van Gurp M., Palmen J. Time temperature superposition for polymeric blends. Rheol Bull. 1998;67:5–8.

[46] Trinkle S., Friedrich C. Van Gurp–Palmen-plot: A way to characterize polydispersity of linear polymers. Rheol. Acta. 2001;40:322–328. DOI: 10.1007/s003970000137

[47] Pötschke P., Abdel-Goad M., Alig I., Dudkin S., Lellinger D. Rheological and dielectrical characterization of melt mixed polycarbonate-multiwalled carbon nanotube composites. Polymer. 2004;45:8863–8870. DOI: 10.1016/j.polymer.2004.10.040

IntechOpen